Kraken : Adaptive Container Provisioning for Deploying Dynamic DAGs in Serverless Platforms

Vivek M. Bhasi
The Pennsylvania State University
vmb5204@psu.edu

Jashwant Raj Gunasekaran
The Pennsylvania State University
jashwant.raj92@gmail.com

Prashanth Thinakaran
The Pennsylvania State University
prashanth.thina@gmail.com

Cyan Subhra Mishra
The Pennsylvania State University
cyan@psu.edu

Mahmut Taylan Kandemir
The Pennsylvania State University
mtk2@psu.edu

Chita Das
The Pennsylvania State University
cxd12@psu.edu

Abstract

The growing popularity of microservices has led to the proliferation of online cloud service-based applications, which are typically modelled as Directed Acyclic Graphs (DAGs) comprising of tens to hundreds of microservices. The vast majority of these applications are user-facing, and hence, have stringent SLO requirements. Serverless functions, having short resource provisioning times and instant scalability, are suitable candidates for developing such latency-critical applications. However, existing serverless providers are unaware of the workflow characteristics of application DAGs, leading to container over-provisioning in many cases. This is further exacerbated in the case of dynamic DAGs, where the function chain for an application is not known a priori. Motivated by these observations, we propose *Kraken*, a workflow-aware resource management framework that minimizes the number of containers provisioned for an application DAG while ensuring SLO-compliance. We design and implement *Kraken* on *OpenFaaS* and evaluate it on a multi-node *Kubernetes*-managed cluster. Our extensive experimental evaluation using *DeathStarbench* workload suite and real-world traces demonstrates that *Kraken* spawns up to 76% fewer containers, thereby improving container utilization and saving cluster-wide energy by up to 4× and 48%, respectively, when compared to state-of-the art schedulers employed in serverless platforms.

CCS Concepts

• **Computer systems organization → Cloud Computing**; *Resource-Management*; Scheduling.

Keywords

serverless, resource-management, scheduling, queuing

1 Introduction

Cloud applications are embracing microservices as a premier application model, owing to their advantages in terms of simplified development and ease of scalability [29, 40]. Many of these real-world services often comprise of tens or even hundreds of loosely-coupled microservices [42] (e.g. Expedia [15] and Airbnb [2]). Typically, these online service applications are user-facing and hence, are administered under strict Service Level Objectives (SLOs) [47, 48] and response latency requirements. Therefore, choosing the underlying resources (virtual machines or containers) from a plethora of public cloud resource offerings [31, 33, 37, 41, 45, 50] becomes crucial due to their characteristics (such as provisioning latency) that determine the response latency. Serverless computing (FaaS) has recently emerged as a first-class platform to deploy latency-critical user facing applications as it mitigates resource management overheads for developers while simultaneously offering instantaneous scalability. However, deploying complex microservice-based applications on FaaS has unique challenges owing to its design limitations.

First, due to the stateless nature of FaaS, individual microservices have to be designed as functions and explicitly chained together using tools to compose the entire application, thus forming a Directed Acyclic Graph (DAG) [33]. Second, the state management between dependent functions has to be explicitly handled using a predefined state machine and made available to the cloud provider [6, 23]. Third, the presence of conditional branches in some DAGs can lead to uncertainties in determining which functions will

be invoked by different requests to the same application. For instance, in a train-ticket application [40], actions like *make_reservation* can trigger different paths/workflows (subset of functions) within the application. These design challenges, when combined with the scheduling and container provisioning policies of current serverless platforms, result in crucial inefficiencies with respect to application performance and provider-side resource utilization. Two such inefficiencies are described below:

• The majority of serverless platforms [32, 44, 46, 50] assume that DAGs in applications are static, implying that all composite functions will be invoked by a single request to the application. This assumption leads to the spawning of equal number of containers for all functions in proportion to the application load, resulting in container over-provisioning.

• Dynamic DAGs, where only a subset of functions within each DAG are invoked per request type, necessitate the apportioning of containers to each function. Recent frameworks like Xanadu [27], predict the most likely functions to be used in the DAG. This results in container provisioning along a single function chain. However, not proportionately allocating containers to all functions in the application can lead to under-provisioning containers for some functions when requests deviate from the predicted path.

To address these challenges, we propose *Kraken*, a DAG workflow-aware resource management framework specifically catered to dynamic DAGs, that minimizes resource consumption, while remaining SLO compliant. The key components of *Kraken* are (i) *Kraken* employs a Proactive Weighted Scaler (PWS) which deploys containers for functions in advance by utilizing a request arrival estimation model. The number of containers to be deployed is jointly determined by the estimation model and function weights. These weights are assigned by the PWS by taking into account function invocation probabilities and parameters pertaining to the DAG structure, namely, *Commonality* (functions common to multiple workflows) and *Connectivity* (number of descendant functions), (ii) In addition to the PWS, *Kraken* employs a Reactive Scaler (RS) to scale containers appropriately to recover from potential resource mismanagement by the PWS, (iii) Further, we batch multiple requests to each container in order to minimize resource consumption.

We have developed a prototype of *Kraken* using *OpenFaaS*, an open source serverless framework [11], and extensively evaluated it using real-world datacenter traces on a 160 core *Kubernetes* cluster. Our results show that *Kraken* spawns up to 76% fewer containers on average, thereby improving container utilization and cluster-wide energy savings by up to 4× and 48%, respectively, when compared to state-of-the art serverless schedulers. Furthermore, *Kraken* guarantees SLO requirements for up to 99.97% of requests.

2 Background and Motivation

We start with providing an overview of serverless DAGs along with related work (Table 1) and discuss the challenges which motivate the need for *Kraken*.

2.1 Serverless Function Chains (DAGs)

Many applications are modeled as function chains and typically administered under strict SLOs (hundreds of milliseconds) [30]. Serverless function chains are formed by stitching together various individual serverless functions using some form of synchronization to provide the functionality of a full-fledged application. Function chains are supported in commercial serverless platforms such as AWS Step Functions [4, 23], IBM Cloud Functions [8], and Azure Durable functions [6]. By characterizing production application traces from Azure, Shahrad et.al [42] have elucidated that 46% of applications have 2-10 functions. Excluding the most general (and rare) cases where applications can have loops/cycles within a function chain [27], applications can be modeled as a *Directed Acyclic Graph* (DAG) where each vertex/stage is a function [26] Henceforth, we will use the terms 'function' and 'stage' interchangeably. We define a *workflow* or *path* within an application as a sequence of vertices and the edges that connect them, starting from the first vertex (or vertices) and ending at the last vertex (or vertices). An application invokes functions in the sequence as specified by the path in the DAG. Based on the nature of the workflow, function chains can be classified as Static or Dynamic.

2.1.1 **Static DAGs** In static function chains (or DAGs), the workflows are specified in advance by the developer (using a schema), which is then orchestrated by the provider. This results in a predetermined path being traversed in the event of an application invocation. For example, in *Hotel Reservation* (Figure 1c), if only one path (say, *NGINX-Make_Reservation*) is always chosen, it represents a static function chain. Henceforth, we refer to static function chains as Static DAG Applications (SDAs). Clearly, having prior knowledge of what functions will be invoked for an application makes container provisioning easier for SDAs.

2.1.2 **Dynamic DAGs** Although the application DAG consists of multiple functions that may be invoked, there are cases where the functions can themselves invoke other functions depending on the inputs they receive. We refer to such functions as Dynamic Branch Points (DBPs), and the chains they are a part of as Dynamic Function Chains. In such cases, deploying containers without prior knowledge about the possible paths in the workflow leads to sub-optimal container provisioning for individual functions. Figure 1 shows the DAGs for three Dynamic Function Chains. *Social Network* (Figure 1a), for example, is one such chain that has 11 functions in total, with each subset of functions contributing to multiple paths (7 paths in total). For instance, from

Features	Archipelago [44]	Power-chief [51]	Fifer [32]	Xanadu [27]	GrandSLAm [34]	Sequoia [46]	Hybrid Histogram [42]	Cirrus [25]	Kraken
SLO Guarantees	✓	✗	✓	✓	✓	✓	✓	✓	✓
Dynamic DAG Applications	✗	✗	✗	✓	✗	✗	✗	✗	✓
Slack-aware batching	✗	✗	✓	✗	✓	✗	✗	✗	✓
Cold Start Spillover Prevention	✗	✗	✗	✗	✗	✗	✗	✗	✓
Function Weight Apportioning	✗	✗	✗	✗	✗	✗	✗	✗	✓
Energy Efficieny	✗	✓	✓	✓	✗	✗	✓	✓	✓
Request Arrival Prediction	✓	✗	✓	✓	✓	✗	✓	✗	✓
Satisfactory Tail Latency	✓	✗	✓	✗	✓	✓	✓	✓	✓

Table 1: Comparing the features of *Kraken* with other state-of-the-art resource management frameworks.

App	DBP	Total Fanout	Possible Paths	Max Depth
Social Network	2	8	7	5
Media Service	3	7	5	6
Hotel Reservation	1	2	2	4

Table 2: Analyzing Variability in Application Workflows.

the start function *NGINX*, any one of *Search*, *Make_Post*, *Read_Timeline* and *Follow* can be taken. Henceforth, we refer to such Dynamic DAG Applications as DDAs.

2.2 Motivation

Two specific challenges in the context of DDAs along with potential opportunities to resolve them are described below:
Challenge 1: Path Prediction in DDAs. DDAs will only have a subset of their functions invoked for an incoming request to the application due to the presence of conditional paths within their DAGs. Figure 1 depicts the DAGs of three such applications from the *DeathStar* benchmark suite [29], and Table 2 summarizes the various workflows that can be triggered by an incoming request to them. 'Total fan-out' and 'Max Depth' denotes the total number of outgoing branches and maximum distance between the start function and any other function in a DAG, respectively. Note that each function triggers only one other function in the application at a time. The decision to trigger the next function typically depends on the input to the current function, although there are cases like *Media Service* where this decision may depend on previous function inputs as well. Therefore, there is considerable variation in the functions that can be invoked in DDAs, thus, negating the inherent assumption in many frameworks [32, 42, 44, 50] that all functions will be invoked with the same frequency as the application. This discrepancy can lead to substantial container overprovisioning.
Opportunity 1: *In order to reduce overprovisioning of containers, it is vital to design a workflow-aware resource management (RM) framework that can dynamically scale containers for each function, as opposed to uniformly scaling for all functions. To design such a policy, the RM framework needs to know each function's invocation frequency, which is a good estimator of its relative popularity.*

We introduce weights to estimate the appropriate number of containers to be spawned for each function. *A function's weight is calculated using the relative invocation frequency of a function along with other DAG-specific parameters* (explained in the next section). The relative invocation frequency of a function is measured with respect to the application it constitutes. The same function belonging to multiple applications can, therefore, have distinct weights in each application.

To analyze the benefits of using invocation frequency, we designed a probability-based policy that employs weighted container scaling. For the purposes of this experiment, we base our function weights only on invocation frequencies that are periodically calculated at the beginning of each scaling window. Figure 2 depicts the number of containers provisioned per function for three container provisioning policies subject to a Poisson arrival trace ($\mu = 25$ requests per second (rps)) for three applications. The static provisioning policy is representative of current platforms [50] which spawn containers for functions in a workflow-agnostic fashion. *Xanadu* [27] represents the policy that scales containers only along the Most Likely Path (MLP), which is the request's expected path. If the request takes a different path, *Xanadu* provisions containers along the path actually taken, in a *reactive* fashion, and scales down the containers it provisioned along the MLP. Consequently, *Xanadu*, when subject to moderate/heavy load, over-provisions containers by 32% compared to the Probability-based policy (from Figure 2) as a result of being locked into provisioning containers for the MLP until it is able to recalculate it. Our probability-based policy, on the other hand, provisions containers for functions along *every possible path in proportion to their assigned weights*. Note that variability in application usage patterns can lead to changes in function probabilities within each DDA, which the policy will have to account for.
Challenge 2: Adaptive Container Provisioning. While probability-based container provisioning can significantly reduce the number of containers, the presence of container cold-starts leads to SLO violations (requests not meeting their expected response latency). This is because cold starts can take up a significant proportion of a function's response time (up to 10s of seconds [13, 14]). A significant amount of research [18, 22, 24, 38, 39, 43, 52] has been focused towards reducing cold-start overheads (in particular, proactive container provisioning [3, 32, 44, 46]). However, in the case of DDAs, DBPs make it unclear as to how many containers should be provisioned in advance for the functions along each path in the DAG.

We identify two interlinked factors, in the context of DDAs, that need to be accounted for when making container scaling decisions. The first, is what we call *critical functions*. These are functions within a DAG that have a high number of descendant functions that are linked to it and we use the
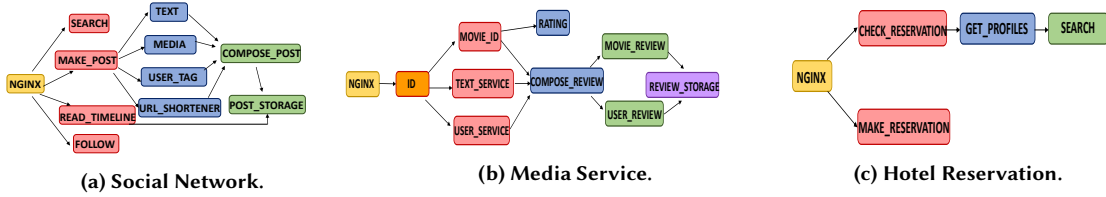
(a) Social Network.   **(b) Media Service.**   **(c) Hotel Reservation.**

Figure 1: DAGs of Dynamic Function Chains.

(a) Social Network.   **(b) Media Service.**   **(c) Hotel Reservation.**
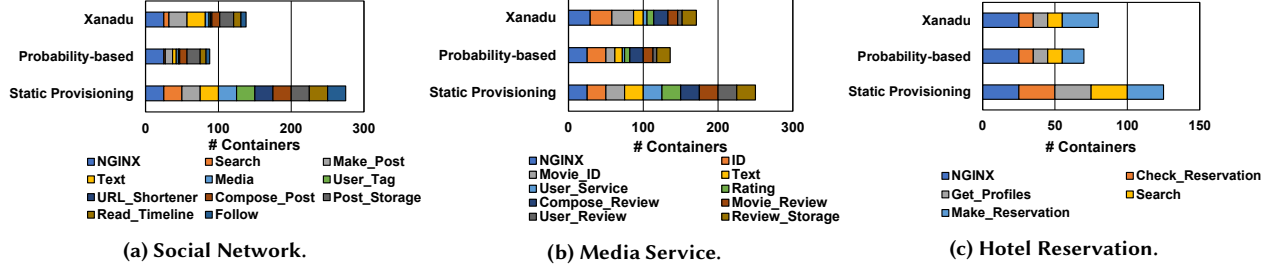
Figure 2: Function-wise Breakdown of Container Provisioning across Applications.
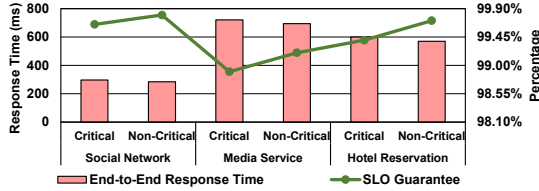

Figure 3: Performance Deterioration resulting from Container Deficiency at Critical Functions. The Primary Y-axis denotes the Average End-to-End Response Time, the Secondary Y-axis represents the percentage of SLOs satisfied and the X-axis indicates the Application under consideration.

term *Connectivity* to denote the ratio of number of descendant functions to the total number of functions. Inadequately provisioning containers for such functions causes requests to queue up as containers are spawned in the background. Moreover, this additional request load trickles down to all the descendants, adversely affecting their response times as well. We refer to this effect as *Cold Start Spillover*. Figure 3 compares the performance degradation resulting from underprovisioning both Critical and Non-Critical functions. The (Critical, Non-Critical) function pairs chosen for this experiment were (*Make_Post*, *Text*), (*ID*, *Rating*) and (*NGINX*, *Search*) for *Social Network*, *Media Service* and *Hotel Reservation*, respectively. It can be observed that underprovisioning containers for just one Critical function has a greater impact on application performance than doing so for a single Non-Critical function, with the end-to-end response time and SLO guarantees becoming 24ms and 0.25% worse on average. This effect can worsen if the same were to happen with multiple critical functions.

In addition to critical functions, it is also crucial to assign higher weights to common functions as well. Common functions refer to those which are a part of two or more paths within an application DAG. Figure 4 shows the 'hit rate' of

functions within an application that is subject to a constant load where any path in the application is equally likely to be picked. It can be seen that functions which are common to a larger number of paths are invoked at a higher rate by such a request arrival pattern. Therefore, common functions have a higher chance of experiencing increased load due to being present in multiple paths. Consequently, higher weights have to be assigned to such functions to ensure resilience in the presence of varying application usage patterns.

Opportunity 2: *Although proactive provisioning combined with probability-based scaling is useful, it is essential to identify critical and common functions in each DDA and assign them higher weights in comparison to standard functions.*
Hence, rather than simply measuring the weights only in terms of function invocation frequency, we also need to account for DAG specific factors like *Commonality* and *Connectivity*. The above discourse motivates us to rethink the design of serverless RM frameworks to cater to DDAs as well. One key driver for the design lies in a *Probability Estimation Model* for individual functions, which is explained below.

3 Function Probability Estimation Model

As elucidated in *Opportunity-1*, to specifically address the container over-provisioning problem for DDAs, we need to estimate the weights to be assigned to their composite functions, a key component of which is the function invocation probability. In this section, we model the function probability estimation problem using a Variable Order Markov Model (VOMM) [21]. VOMMs are effective in capturing the invocation patterns of functions within each application while simultaneously isolating the effects of other applications that share them. This aids us in the calculation of function invocation probabilities. Wherever appropriate, we draw inspiration from related works that model user web surfing
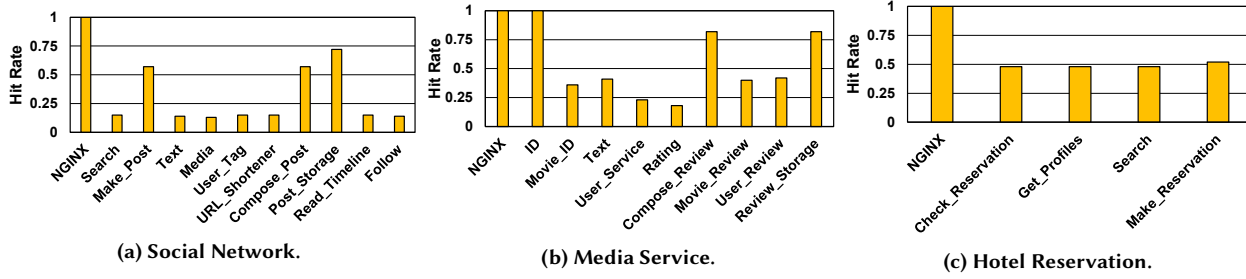
(a) Social Network.   (b) Media Service.   (c) Hotel Reservation.

Figure 4: Function Hit Rate for an Evenly Distributed Load across all Paths in each Application.
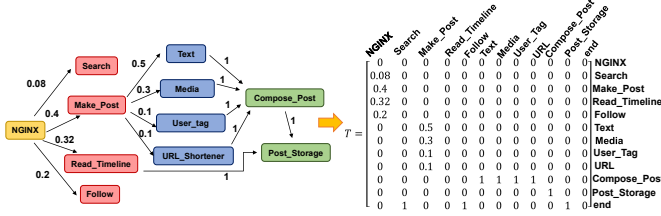

Figure 5: Transforming the Social Network DAG into a Transition Matrix.

behavior [19, 20]. VOMMs are an extension of Markov Models [28], where the transition probability from the current state to the next state depends not only on the current state, but possibly on its predecessors (which we refer to as the 'context' of the state). Such behavior is seen in some of our workloads such as *Media Service*. The order of the VOMM denotes the number of predecessors that influence the transition decision.

An application DAG can map neatly onto a Markov model wherein the functions within the application DAG are modeled as states of the VOMM. The process of one function invoking another function corresponds to a transition from the caller function state to the callee function state. The weight for each function corresponds to the state transition probability from the start state to the current one (note that this may require possibly transitioning through a number of intermediate states).

Thus, for a DAG with n functions, the transition probability matrix, T, is an $n \times n$ matrix, where n is the total number of states and each entry, $t_{j\,i}$, is the transition probability from the state corresponding to the function along the column j, (f_j), to that of the function along the row i, (f_i). An example of a Transition Matrix for the *Social Network*, with 11 functions, is depicted in Figure 5. An additional state, *end*, is added to represent the state the model transitions to after a path in the DAG is completely executed. In Figure 5, assuming both column and row indices of T start at 0, an entry $t_{0\,4}$ represents the transition probability from *NGINX*'s state to *Follow*'s state and is equal to 0.2. In general, this transition probability, $t_{j\,i}$, is calculated as the number of requests from f_j to f_i divided by the number of incoming requests to f_i in the context of the application being considered.

The Probability Vector is an $n \times 1$ column vector that captures the probabilities of the model being in different states after a number of time steps have elapsed, given that the model was initialized at a known state. A 'time step' refers to a unit of measuring state change in the Markov Model. For practical purposes, we fix it to be the execution time of the slowest function at the current function depth. The 'depth' of a function, in this context, is defined as the distance, in terms of the number of edges in the DAG, from the start state to the current state. The Probability Vector after d number of time steps can be represented as P_d. Then, the Probability Vector for the next time step, $d + 1$, is given by the *transition equation*, $P_{t+1} = T \cdot P_t$. This equation infers that the Probability Vector at the next time step is obtained by performing a transition operation across all possible current states.

Repeatedly carrying out this transition process, starting from the initial Probability Vector, enables the estimation of probabilities of each function along all possible workflows. Iterating this process for d time steps would yield the probabilities of functions at a depth of d from the start function, given by $P_d = T^d \cdot P_0$. Thus, we can compute the probability of any function in the DAG by varying the depth, d, using this equation. In order to apply this to proactive container allocation decisions, we can adopt the following procedure.

The incoming load to the application at time stamp, t, is denoted as PL_t and can be predicted using a load estimation model. Assuming each request to a function within the application spawns one container for that function, the number of containers to be provisioned in advance for functions at depth d is given by:

$$NC_t^d = \lceil PL_t \cdot (T^d \cdot P_0) \rceil$$

Here, NC_t^d is a column vector of n elements, each corresponding to the number of elements required to be provisioned for functions at a depth, d, from the start function. Provisioning these containers at a fixed time window in advance from t prevents cold starts from affecting the end-user experience. For example, if PL_t is estimated to be 25 requests, then from Figure 5, we obtain the number of containers needed for functions at depth, $d = 1$, by multiplying 25 with P_1 (which is $T^1 \cdot P_0$). Consequently, the total number of containers required for each function in the application can be computed

Notation	Meaning
T	Transition Matrix
P_d	Probability Vector for functions at depth, d
n	# functions in application or # states in model
f_i, f_j	functions along row, i or column, j in T
$t_{j\,i}$	Transition probability from f_j to f_i
W_p	Probability calculation time window
t	Request arrival time
d	# time steps for which transitions are done
PL_t	Scalar that represents the anticipated # requests at time, t
NC_t^d	# containers needed for functions at depth d, at time t

Table 3: Notations used in Equations.

by performing a summation of NC_t^d across all possible depths, d, from the start function.

We can now transform our previously-assumed Markov Model into a VOMM by splitting up context-dependent states into multiple context-independent states (the number of which is dependent on the DAG structure and the order of the VOMM). For example, in Figure 5, if the transition from *Compose_Post* to *Post_Storage* depended on the immediate predecessors of *Compose_Post*, the *Compose_Post* state would be context-dependent and would therefore, be split into context-independent states, namely, $Compose\_Post|Text$ (*Compose Post* given $Text$ was already invoked), $Compose\_Post|Media$ etc. for the previous equations to hold. This changes the total number of states from n to N, the number of extended states, resulting in a larger Transition Matrix and Probability Vector. To calculate the required number of containers for a single function that has multiple context-independent states associated with it, we take the sum of the calculated values for all of those states.

4 Overall Design of Kraken

Kraken[1] leverages the function weight estimation model from the above section along with several other design choices as outlined in this section (Figure 6). Users submit requests in the form of invocation triggers to applications ❶ hosted on a Serverless platform. In *Kraken*, containers are provisioned in advance by the Proactive Weighted Scaler (PWS) ❷ to serve these incoming requests by avoiding cold starts. To achieve this, the PWS ❷ first fetches relevant system metrics (using a monitoring tool ❸ and orchestrator logs). These metrics, in addition to a developer-provided DAG Descriptor ❹, are then used by the Weight Estimation module ❷ₐ of PWS ❷ to assign weights to functions on the basis of their invocation probabilities. *Commonality* and *Connectivity* (parameters in ❷ₐ) are additional parameters used in weight estimation to account for critical and common functions. Additionally, a Load Predictor module ❷ᵦ makes use of the system metrics to predict

---

[1]Kraken is a legendary sea monster with tentacles akin to multiple paths/chains in a Serverless DAG.
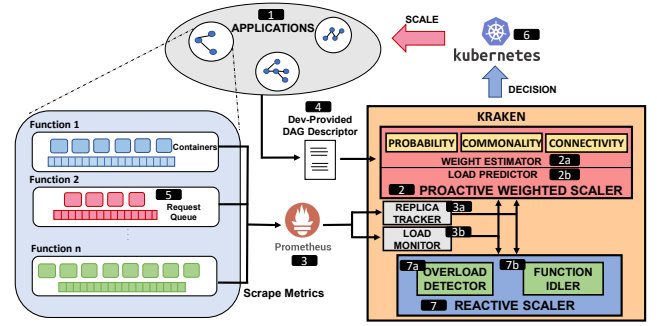

Figure 6: High-level View of Kraken Architecture

incoming load and uses this in conjunction with the calculated function weights to determine the number of function containers to be spawned by the underlying resource orchestrator ❻. However, only a fraction of these containers are actually spawned, as determined by the function's batch size. The batch size denotes the number of requests per function each container can simultaneously serve without exceeding the SLO. In order to effectively handle mis-predictions in load, *Kraken* also employs a Reactive Scaler (RS) ❼ that consists of two major components. First, is an Overload Detector ❼ₐ that keeps track of request overloading at functions by monitoring queuing delays at containers. Subsequently, it triggers container scaling ❻ by calculating the additional containers needed to mitigate the delay. Second, a Function Idler component ❼ᵦ evicts containers from memory ❻ when an excess is detected. Thus, *Kraken* makes use of PWS and RS to scale containers to meet the target SLOs while simultaneously minimizing the number of containers by making use of function invocation probabilities, function batching, and container eviction, where appropriate.

4.1 Proactive Weighted Scaler

We describe in detail the components of PWS below.

4.1.1 ***Estimating function weights*** Since workflows in SDAs are pre-determined, pre-deploying resources for them is straightforward in comparison to DDAs, whose workflow activation patterns are not known a priori. For DDAs, deploying containers for each function in proportion to the application load will inevitably lead to resource wastage. To address this, we design a Weight Estimator ❷ₐ to assign weights to all functions so as to allocate resources in proportion to them. Explained below is the working of the procedure *Estimate_Containers* in Algorithm 1 which is used to estimate function weights.

Probability: As alluded to in Section 2, one of the factors used in function weight estimation is its invocation probability. The procedure in Section 3 describes how the transition probabilities of the states associated with functions are computed through repeated matrix multiplications of the Transition Matrix, T with the Probability Vector, P. *Compute_Prob*,

in Algorithm 1, first estimates the invocation probabilities of a function's immediate predecessors and uses it along with system log information and load measurements of the function to calculate its invocation probability.

Connectivity: In addition to function invocation probabilities, it is necessary to also account for the effects of cold starts on DDAs while estimating function weights. Cold start spillovers (that often occur due to container underprovisioning), as described in Section 2, can impact the response latency of applications harshly. Provisioning critical functions with more containers helps throttle this at the source. To this end, *Kraken* makes use of a parameter called *Connectivity*, while assigning function weights. The *Connectivity* of a function is defined as the ratio of number of its descendant functions to the total number of functions. The *Conn* procedure in Algorithm 1 makes use of this formula. For example, in Figure 1c, the *Connectivity* of *Check_Reservation* is $\frac{2}{5}$ since it has two descendants and there is a total of five functions. Bringing *Connectivity* into the weight estimation process helps *Kraken* assign a higher weight to critical functions, in turn, ensuring that more containers are assigned to them, resulting in improved response times for the functions themselves, as well as their descendants.

Commonality: As described in Section 2, in addition to cold start spillovers, incorrect probability estimations may arise due to variability in workflow activation patterns. This may be due to change in user behavior manifesting itself as variable function input patterns. Such errors can lead to suboptimal container allocation to DAG stages in proportion to the wrongly-calculated function weights. To cope with this, we introduce a parameter called *Commonality*, which is defined as the fraction of number of unique paths that the function can be a part of with respect to the total number of unique paths. This is how the procedure *Comm* calculates *Commonality* in Algorithm 1. For example, in Figure 1a, the *Commonality* of the function *Compose_Post* in the *Social Network* application is given by the fraction $\frac{4}{7}$ as it is present in four out of the seven possible paths in the DAG. Using *Commonality* in the weight estimation process allows *Kraken* to tolerate function probability miscalculations by assigning higher weights to those functions that are statistically more likely to experience rise in usage because of their presence in a larger number of workflows. Note that we deal with the possibility of container overprovisioning due to the increased function weights by allowing both *Connectivity* and *Commonality* to be capped at a certain value.

4.1.2 ***Proactive Container Provisioning*** Once function weights are assigned by considering the above factors, they are employed in estimating the number of containers needed per DAG stage (*Estimate_Containers* in Algorithm 1). These containers have to be provisioned in advance to service future load to shield the end user from the effects of cold starts

and thereby meet the SLO. This load will have to be predicted in order to make timely container provisioning decisions.

Algorithm 1 Proactive Scaling with weight estimation

1: **for** *Every Monitor_Interval= PW* **do**
2:     ***Proactive_Weighted_Scaler***$(\forall functions)$

3: **procedure** Proactive_Weighted_Scaler(*FUNC*)
4:     $cl \leftarrow Current\_Load(func)$
5:     $pl_{t+PW} \leftarrow$ ***Load_Predictor***(cl, pl_t) **ⓐ**
6:     $batches \leftarrow \left\lceil \frac{pl_{t+PW}}{func.batch\_size} \right\rceil$ **ⓑ**
7:     $total\_con \leftarrow$ ***Estimate_Containers***$(batches, func)$
8:     $reqd\_con \leftarrow max(min\_con, total\_con)$
9:     ***Scale_Containers***$(func, reqd\_con)$

10: **procedure** estimate_containers(*LOAD, FUNC*)   ▷ Output: *reqd_con*
11:     $func.prob \leftarrow$ ***Compute_Prob***$(func)$
12:     $reqd\_con \leftarrow \lceil load * func.prob \rceil$
13:     $extra \leftarrow \lceil (\textbf{\textit{Comm}}(func) + \textbf{\textit{Conn}}(func)) * reqd\_con \rceil$
14:     $reqd\_con \leftarrow reqd\_con + extra$

Kraken makes use of a Load Predictor **②ⓑ** (Algorithm 1 **ⓐ**) which uses the EWMA model to predict the incoming load at the end of a fixed time window, *PW*. This time window is chosen according to the time taken to scale all functions in the respective application. Note that *t* in the algorithm refers to the current time. We choose this model so as to have a light-weight load prediction mechanism that has minimal impact on the end-to-end latency ($\sim 10^{-3}$ ms). This Load Predictor **②ⓑ** can be used in conjunction with the aforementioned Weight Estimator **②ⓐ** to calculate the fraction of application load each function will receive. *Kraken* uses this load distribution to pre-provision the requisite number of containers for all functions in the application.

4.2 Request Batching

Many serverless frameworks [5, 10, 17, 27, 44, 46, 50] spawn a single container to serve each incoming request to a function. While this approach is beneficial to minimize SLO violations, comparable performance can be achieved by using fewer containers by leveraging the notion of slack [32, 34]. Slack refers to the difference in expected response time and actual execution time of functions within a function chain. Functions in a chain can have widely varying execution times. Allotting stage-wise SLOs to each function in a chain in proportion to their execution times reveals that there are cases where there is significant difference (slack) between the function's expected SLO and its run-time. Figure 7 depicts this slack for all functions in the applications considered.

This slack is leveraged by *Kraken* by batching multiple requests to the functions by queueing requests at their containers. Requests are batched onto containers in a fashion similar to the First Fit Bin Packing algorithm [36]. Batching reduces the number of containers spawned for each function by a factor of its batch size (Algorithm 1 **ⓑ**). The batch size for a function, f, is defined as $BatchSize(f) = \left\lfloor \frac{StageSLO(f)}{ExecTime(f)} \right\rfloor$ (Algorithm 1 **ⓑ**). Note that *ExecTime (f)* is estimated by averaging the execution times of the function obtained through
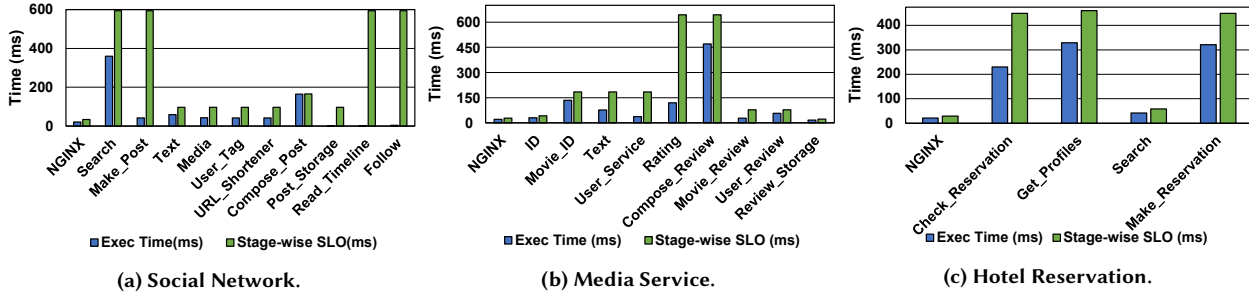
Figure 7: Slack for various Functions in each Application.

offline profiling and *StageSLO (f)* is allotted in proportion to it. The batch size represents the number of requests that can be served by a function without violating the allotted stage-wise SLO.

4.3 Reactive Scaler (RS)

Though the introduction of Request Batching ❺ allows *Kraken* to reduce the containers provisioned, load mispredictions and probability miscalculations can still occur, leading to resource mismanagement, which could potentially affect the SLO compliance. To deal with this, *Kraken* also employs the RS ❼ to scale containers up or down in response to request overloading at containers (due to under-provisioning) and container over-provisioning, respectively.

In case of inadequate container provisioning, the Overload Detector ❼ⓐ in the RS ❼ detects the number of allocated containers for each DAG stage and calculates the estimated wait times of their queued requests (Algorithm 2 ❺ⓑ). If it detects requests whose wait times exceed the cost of spawning a new container (the cold start of the function), overloading is said to have occurred at the stage. In such a scenario, *Kraken* batches these requests (*#_delayed_requests* in Algorithm 2) onto a newly-spawned container(s) (Algorithm 2 ⓒ). This is because requests that have to wait longer than the cold start would be served faster at a newly created container than by waiting at an overloaded container. Similarly, for stages where container overprovisioning has occurred, the RS ❼ gradually scales down its allocated containers to the appropriate number, if its Function Idler module ❼ⓑ detects excess containers for serving the current load (Algorithm 2 ⓐ). Thus, the RS ❼, in combination with the PWS ❷ and request batching ❺, helps *Kraken* remain SLO compliant while using minimum resources.

5 Implementation and Evaluation

We have implemented a prototype of *Kraken* using open-source tools for evaluation with synthetic and real-world traces. The details are described below.

5.1 Prototype Implementation

Kraken is implemented primarily using Python and Go on top of *OpenFaaS* [11], an open-source serverless platform.

Algorithm 2 Reactive Scaling

1: **for** *Every Monitor_Interval= DR* **do**
2:     ***Reactive_Resource_Manager(∀functions)***
3: **procedure** REACTIVE_RESOURCE_MANAGER(*FUNC*)
4:     $cl \leftarrow Current\_Load(func)$
5:     $func.existing\_con \leftarrow Current\_Replicas(func)$
6:     **if** $\left\lceil \frac{cl}{func.batch\_size} \right\rceil \leq func.existing\_con$ **then** ⓐ
7:         $reqd\_con \leftarrow \left\lceil \frac{cl}{func.batch\_size} \right\rceil$
8:     **else**
9:         $\#\_delayed\_requests \leftarrow Delay\_Estimator(func)$ ⓑ
10:         $extra\_con \leftarrow \left\lceil \frac{\#\_delayed\_requests}{func.batch\_size} \right\rceil$ ⓒ
11:         $reqd\_con \leftarrow func.existing\_con + extra\_con$
12:     ***Scale_Containers***$(func, reqd\_con)$

OpenFaaS is deployed on top of *Kubernetes* [9], which acts as the chief container orchestrator. *OpenFaaS*, by default, comes packaged with an Alert Manager module which is responsible for alerting the underlying orchestrator of request surges by using metrics scraped by *Prometheus*, which is an open-source systems monitoring toolkit [12]. This, in turn, triggers autoscaling to provision extra containers to service the load surge. We disable this Alert Manager and deploy the Proactive Weighted Scaler (PWS) and Reactive Scaler (RS) to carry out our container provisioning policies.

Both the PWS and RS collect metrics, such as the current container count, load history and request rate for a function for a given time window, from *Prometheus* and the *Kubernetes* system log, using the Replica Tracker and Load Monitor modules. Although fetching function metrics incurs a latency in the order of tens of milliseconds, it is performed in the background (during autoscaling) and hence, does not affect the critical path. The load to each function within each application is calculated separately using the collected information. This prevents other applications from interfering with the probability calculation of shared functions. Additionally, the PWS uses a DAG descriptor, which is a file that contains a python dictionary that specifies the connectivity among functions. Although constructing this is a one-time effort, automating this process through offline DAG profiling can be explored in future work. Table 4 gives an overview of *Kraken*'s policies and their implementation details.

Policy	Component	Implemented using/as
PWS	Probability *Commonality & Connectivity* Load Predictor	System log info, Sparse Data Structures DAG Descriptor Pluggable model (EWMA)
Batching		Function containers persisted in memory
RS	Load Monitor Replica Tracker	Metrics from Prometheus & System logs

Table 4: Implementation details of *Kraken*'s policies.

5.2 Evaluation Methodology

We evaluate the *Kraken* prototype on a 5 node *Kubernetes* cluster with a dedicated manager node. Each node is equipped with, 32 cores (Intel CascadeLake), 256GB of RAM, 1 TB of storage and a 10 Gigabit Ethernet interconnect [35]. For energy measurements, we use an open-source version of Intel Power Gadget [16] that measures the energy consumed by all sockets in a node.

Load Generator: We provide different traces as inputs to a load generator, which is based on Hey, an HTTP Load generator tool [7]. First, we use a synthetic Poisson-based request arrival rate with an average rate $\mu = 100$. Second, we use real-world request arrival traces from Wiki [49] and Twitter [1] by running each experiment for about an hour. The Twitter trace has a large variation in peaks (average = 3332 rps, peak= 6978 rps) when compared to the Wiki trace (average = 284 rps, peak = 331 rps).

Applications: Each request is modeled after a query to one of the three applications (DDAs) we consider from the *DeathStar* benchmark suite [29]. We implement each application as a workflow of chained functions in *OpenFaaS*. To model the characteristics of the original functions, we invoke sleep timers within our functions to emulate their execution times (including the time for state recovery, if any). Transitions between functions are done using function calls on the basis of pre-assigned inter-function transition probabilities. The probabilities vary by approximately ±20% of a seed. Note that these probabilities are not visible to *Kraken*, but are only used to model function invocation patterns.

Metrics and Resource Management Policies: We use the following metrics for evaluation: (i) average number of containers spawned, (ii) percentage of requests satisfying the SLO (SLO guarantees), (iii) average application response times, (iv) end-to-end request latency percentiles, (v) container utilization, and (vi) cluster-wide energy savings. We set the SLO at 1000ms. We compare these metrics for *Kraken* against the container provisioning policies of Archipelago [44], *Fifer* [32] and *Xanadu* [27], which we will, henceforth, refer to as *Arch*, *Fifer* and *Xanadu*, respectively. Additionally, we compare *Kraken* against policies with (a) statically assigned function probabilities (*SProb*) and (b) function probabilities that dynamically adapt to changing invocation patterns (*DProb*). These policies use all the components of *Kraken* except *Commonality* and *Connectivity*.

5.3 Large Scale Simulation

To evaluate the effectiveness of *Kraken* in large-scale systems, we built a high fidelity, multi-threaded simulator in Python using container cold start latencies and function execution times profiled from our real-system counterpart. It simulates the working of DDAs running on a serverless framework that are subjected to both real-world (Twitter and Wiki) and synthetic (Poisson-based) traces. We have validated its correctness by correlating various metrics of interest generated from experiments run on the real system with scaled-down versions of the same traces (average arrival rate of ~100rps). Therefore, the simulator allows us to evaluate our model for a larger setup, where we mimic an 11k core cluster which can handle up to 7000 requests (70× more than the real system). Additionally, it helps compare the resource footprint of *Kraken* against a clairvoyant policy (Oracle) that has 100% load prediction accuracy.

6 Analysis of Results

This section presents experimental results for single applications run in isolation for all schemes on the real system and simulation platform. We have also verified that *Kraken* (as well as the other schemes) yield similar results (within 2%) when multiple applications are run concurrently.

6.1 Real System Results

*6.1.1 **Containers Spawned** Figure 8 depicts the function-wise breakdown of the number of containers provisioned across all policies for individual applications. This represents NC_t^d (Section 3) for all possible depths, d. It can be observed that, existing policies, namely, *Arch*, *Fifer* and *Xanadu* spawn, respectively, 2.41x, 76% and 30% more containers than *Kraken*, on average, across all applications. Overallocation of containers in case of *Arch* is due to two reasons: (i) it assumes that all functions in the application will be invoked at runtime; and (ii) it spawns one container per invocation request. On the other hand, *Fifer* improves upon this by reducing the total number of containers spawned using request batching. However, it does not take workflow activation patterns into consideration while spawning containers, leading to container overprovisioning. The recently proposed scheme, *Xanadu*, is based on a workflow-aware container deployment mechanism, but does not employ request batching, leading to extra containers being deployed in comparison to *Kraken*. Furthermore, it can be seen that *Xanadu* provisions a relatively high number of containers for a particular group of functions as compared to the rest. This is because it allocates containers to serve the predicted load along only the Most Likely Path (MLP) of a request. The rest of the containers are a result of *reactive scaling* that follows from MLP mispredictions, which accounts for 34% of the total number of containers spawned.
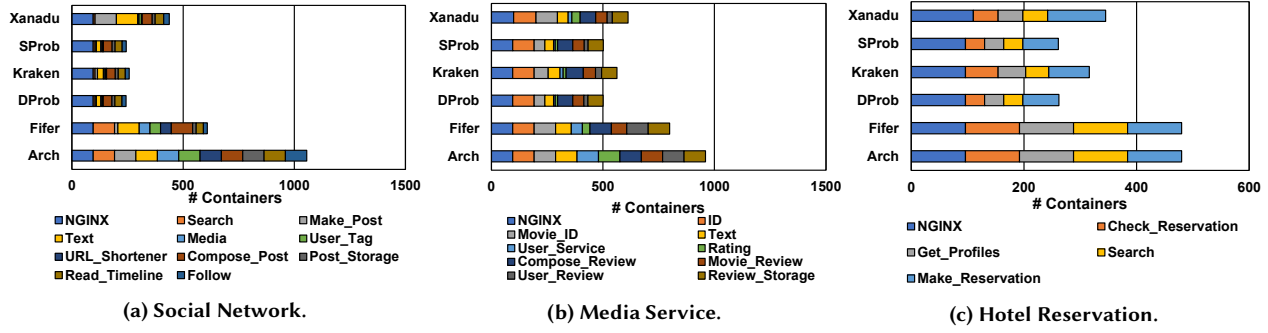
(a) Social Network. (b) Media Service. (c) Hotel Reservation.

Figure 8: Real System: Stage-wise Breakdown of Containers spawned by each policy.

The reduction in the number of containers spawned by *Kraken* in comparison to other policies is roughly proportional to the total number of application workflows and the slack available for each function within a workflow (see Table 2 and Figure 7). For instance, Figure 8 indicates that the *Social Network*, *Media Service* and *Hotel Reservation* applications show the highest (73%, 53% and 36%), moderate (40%, 28% and 7%) and least (at most 33%) reductions in the number of containers spawned with respect to existing policies, *Arch*, *Fifer* and *Xanadu*, respectively. Both *Social Network* and *Media Service* have a high number of workflows, but the former has more functions with higher slack, leading to increased batching, thereby resulting in the most reduction in containers spawned. *Hotel Reservation* has the least number of workflows as well as the lowest overall slack for all functions, resulting in the least reduction in the number of containers. On the other hand, *DProb* and *SProb* spawn fewer containers than *Kraken* as a consequence of not using *Commonality* and *Connectivity* to augment function weights, while making container allocation decisions. As a result, *Kraken* provisions up to 21% more containers than both *DProb* and *SProb* for the three applications. Note that, these additional containers are necessary to reduce SLO violations.

*6.1.2 **End-to-End Response Times and SLO Compliance*** Figure 9 shows the breakdown of the average end-to-end response times and Figure 10 juxtaposes the total number of containers provisioned against the SLO Guarantees for all policies and applications, averaged across all traces. From these graphs, it is evident that *Kraken* exhibits comparable performance to existing policies while having a minimal resource footprint. For the *Social Network* application, *Kraken* remains within 60 ms of the end-to-end response time of *Arch* (Figure 9a), which performs the best out of all policies with respect to these metrics, while ensuring 99.94% SLO guarantees (Figure 10a) . However, *Arch* uses 4x the number of containers used by *Kraken* (Figure 10a).

Kraken also performs similar to *Fifer*, while using 58% reduced containers for *Social Network*. From Figures 9 and 10, it can be seen that *Xanadu* has similar (or worse) end-to-end response times than *Kraken* (up to 50 ms more), but

spawns more containers as well (up to 70% more) and satisfies fewer SLOs on average (0.2% lesser). This can be attributed to *Xanadu*'s container pre-deployment policy which causes reactive scale outs as a result of MLP mispredictions. This effect is highlighted in applications such as *Social Network* and *Media Service* which have relatively high MLP misprediction rates (80% and 50%, respectively[2])) due to the presence of multiple possible paths (Table 2). *Media Service* suffers from higher end-to-end response times, further exacerbating this effect. *Xanadu* has only a 34% misprediction rate for *Hotel Reservation*, due to the lower number of workflows, and is seen to match *Kraken* in terms of SLOs satisfied (99.87%).

The breakdown of the average response times in Figure 9 shows that both *Arch* and *Xanadu* do not suffer from queueing delays. This is because both policies spawn a container per request, resulting in almost zero queueing. The relatively high cold start-induced delay experienced by *Xanadu* can be attributed to the reactive scaling it uses to cope with MLP mispredictions. *Kraken* exhibits delay characteristics similar to *Fifer* owing to both policies having batching and a similar container pre-deployment policy. However, *Kraken* allocates fewer containers (57% lesser, on average across all applications) along each workflow compared to *Fifer*. *DProb* and *SProb* exhibit higher overall end-to-end response times compared to *Kraken*, with *SProb* experiencing a disproportionately high queueing delay compared to its cold start delay. This is because it uses statically assigned function weights, which prevents it from being able to proactively spawn containers according to the varying user input. This results in the majority of requests getting queued at the containers.

*6.1.3 **Analysis of Key Improvements*** This subsection focuses on the key improvements offered by *Kraken* in terms of Container Utilization, Response Latency Distribution and Energy Efficiency. Although we use specific combinations of applications and traces to highlight the improvements, the results are similar for other workload mixes as well.

Container Utilization: Figure 11 plots the average number of requests executed per container (Jobs per container)

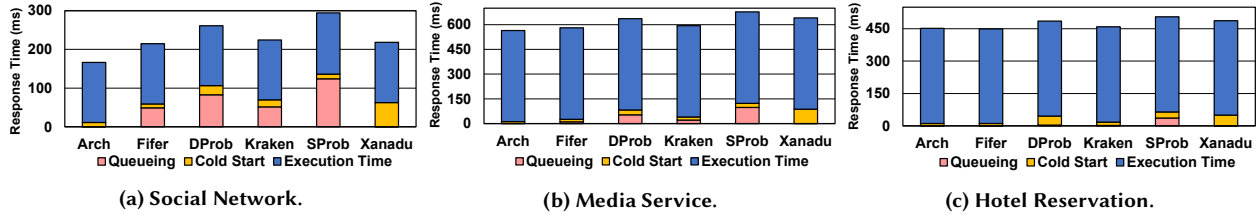[2]MLP misprediction rates are not shown in any Figure

(a) Social Network.　　　　　　　　(b) Media Service.　　　　　　　　(c) Hotel Reservation.

Figure 9: Real System: Breakdown of Average End-to-End Response Times in terms of queueing delay, cold start delay and execution time.

(a) Social Network.　　　　　　　　(b) Media Service.　　　　　　　　(c) Hotel Reservation.
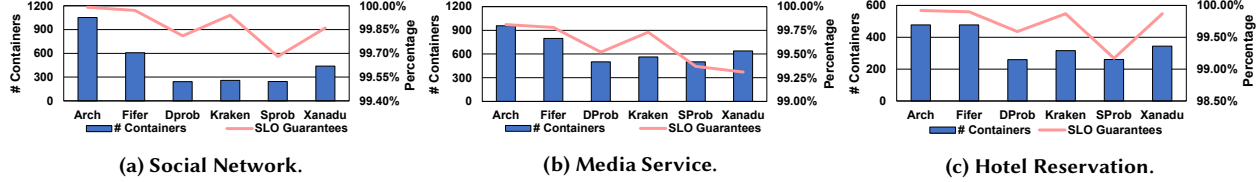
Figure 10: Real System: Comparison of Total Number of Containers spawned VS SLOs satisfied by each policy. The Primary Y-Axis denotes the number of containers spawned, The secondary Y-axis indicates the percentage of SLOs met and the X-axis represents each policy.
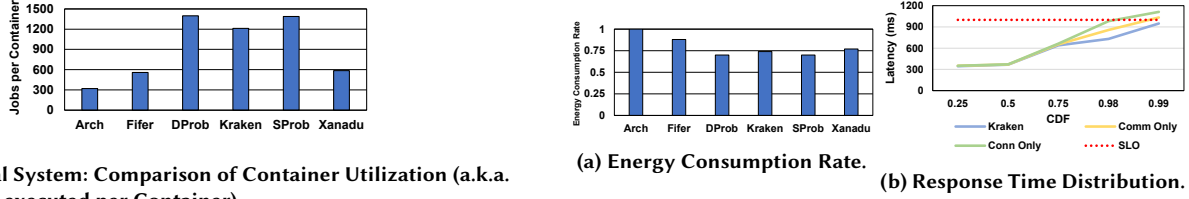

Figure 11: Real System: Comparison of Container Utilization (a.k.a. average #jobs executed per Container).
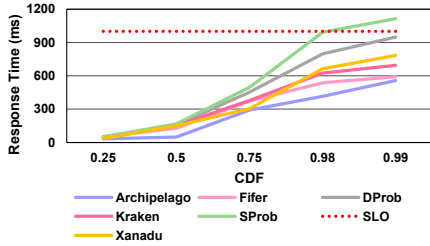

Figure 12: Real System: Response Time Distribution.

(a) Energy Consumption Rate.

(b) Response Time Distribution.

Figure 13: Real System: Normalized Energy Consumption of all Schemes and Response Time Distribution of *Kraken*, *Comm Only* and *Conn Only*

across all functions in *Social Network* for the Poisson trace. An ideal scheme would focus on packing more number of requests per container to improve utilization without causing SLO violations. *Kraken* shows 4x, 2.16x and 2.06x more container utilization compared to *Arch*, *Fifer*, and *Xanadu* respectively. This is because *Kraken* limits the number of containers spawned through function weight assignment and request batching. *DProb* and *SProb* both exhibit higher utilization compared to *Kraken* (15%) as a result of spawning fewer containers overall, owing to not accounting for *critical* and *common* functions while provisioning containers. Consequently, they exhibit up to 0.24% more SLO Violations compared to *Kraken*, for this workload mix.

Latency Distribution: The end-to-end latency distribution for all policies for the *Social Network* application with the Twitter trace is plotted in Figure 12. In particular, *Arch*, *Fifer* and *Kraken* show comparable latencies, with P99 values remaining well within the SLO of 1000ms. However, *Arch* and *Fifer* use 3.51x and 2.1x more containers than *Kraken* to

achieve this. The tail latency (measured at P99) for *DProb* almost exceeds the SLO, whereas it does so for *SProb*. *Kraken* manages to avoid high tail latency by assigning augmented weights to key functions, thus, helping it tolerate incorrect load/probability estimations. *SProb* does worse than *DProb* at the tail because of its lack of adaptive probability estimation. *Kraken* makes use of 21% more containers to achieve the improved latencies. *Xanadu* experiences a sudden rise in tail latency, with it being 100ms more than that of *Kraken*, while using 96% more containers. This is due to *Xanadu*'s MLP misprediction and the resultant container over-provisioning.

Energy Efficiency: We measure the energy-consumption as total Energy consumed divided over total time. *Kraken* achieves one of the lowest energy consumption rates among all the policies considered, with it bettering existing policies, namely, *Arch*, *Fifer* and *Xanadu* by 26%, 14% and 3% respectively (for the workload mix of *Media Service* application with Wiki trace) as depicted in Figure 13a. These savings can go up to 48% compared to *Arch* for applications like *Social Network*. The resultant energy savings of *Kraken* are a direct consequence of the savings in computation and memory usage from the fewer containers spawned. Only *DProb* and *SProb* consume lesser energy than *Kraken* (4% lesser), due to their more aggressive container reduction approach.

6.1.4 ***Ablation Study*** This subsection conducts a brick-by-brick evaluation of *Kraken* using *Conn Only* and *Comm Only*,

Application	Kraken	Comm Only	Conn Only
Social Network	(99.94%, 284)	(99.91%, 276)	(99.89%, 256)
Media Service	(99.73%, 572)	(99.66%, 561)	(99.64%, 552)
Hotel Reservation	(99.87%, 316)	(99.77%, 290)	(99.74%, 282)

Table 5: Real System: Comparing (SLO Guarantees,#Containers Spawned) against *Comm Only* and *Conn Only*.

Policy	Poisson		Wiki		Twitter	
	Med	**Tail**	**Med**	**Tail**	**Med**	**Tail**
Arch	336	568	336	568	336	599
Fifer	362	612	360	611	373	833
DProb	371	746	368	753	381	1549
Kraken	366	634	358	633	371	974
SProb	395	1101	382	1073	395	1610
Xanadu	343	723	340	774	340	1244

Table 6: Simulator: Median and tail latencies (in ms) averaged across all applications for the three traces

schemes that exclude *Commonality* and *Connectivity* components from *Kraken*, respectively. From Table 5, it can be seen that *Comm Only* spawns 8% more containers than *Conn Only* for *Social Network*. This difference is lesser for the other applications. Upon closer examination, we see that this is due to functions having different degrees of *Commonality* and *Connectivity*. Moreover, the majority of functions whose *Commonality* and *Connectivity* differ, have a high batch size, thereby reducing the variation in the number of containers spawned. Following this, we observe that the variation in the number of containers in *Social Network* is mainly due to the significant difference in the *Commonality* and *Connectivity* of the *Compose Post* function whose batch size is only one. There is lesser difference in containers spawned by *Comm Only*, *Conn Only* and *Kraken* for *Media Service* because we have implemented *Kraken* with a cap on the additional containers spawned due to *Commonality* and *Connectivity* when the sum of their values exceeds a threshold. This threshold is exceeded in *Media Service* for the majority of functions. Due to the difference in container provisioning, the difference in response times between the three schemes is evident at the tail of the response time distribution (Figure 13b). *Comm Only* and *Conn Only* are seen to exceed the target SLO at the 99th percentile. The tail latency of *Kraken*, in comparison, grows slower and remains within the target SLO.

6.2 Simulator Results

Since the real-system is limited to a 160-core cluster, we use our in-house simulator, which can simulate an 11k-core cluster, to study the scalability of *Kraken*. We mimic a large scale Poisson arrival trace (μ = 1000rps), Wiki (μ = 284 rps) and Twitter (μ = 3332 rps) traces. Figure 14 plots the containers spawned versus the SLO guarantees for each application for all traces. The simulator results closely correlate to those of the real system. *Kraken* is seen to reduce container overprovisioning when applications have numerous possible workflows and enough slack per function to exploit. Notably, *Kraken* spawns nearly 80% less containers for *Social Network* in comparison to *Arch*. Container overprovisioning is inflated 15% more than the corresponding real system result, due to the large-scale traces. Table 6 shows the median and tail latencies of each policy averaged across all applications for the three traces. The trend we observe is that traces with higher variability, such as the Twitter trace, affect the tail latencies of policies more harshly than the other, more predictable, traces. Nevertheless, *Kraken* is resilient to

unpredictable loads as well, with tail latencies always remaining within the SLO (1000 ms). However, the tail latencies of *DProb* and *SProb* sometimes exceeds the SLO, since they don't use *Commonality* and *Connectivity*. It is observed that *Xanadu* also violates the SLO for the Twitter trace, owing to the reactive scale-outs resulting from MLP mispredictions.

6.2.1 Sensitivity Study This subsection compares *Kraken* against *Oracle*, which is an ideal policy that is assumed to be able to predict future load and all path probabilities with 100% accuracy and also has request batching. Consequently, *Oracle* does not suffer from cold starts and minimizes containers spawned. Figure 15 shows the breakdown of total number of containers spawned for each application, averaged across all realistic large-scale traces using the simulator. It is observed that *Kraken* spawns more containers (7%) than *Oracle*, on average. This is due to *Kraken*'s load/path probability miscalculations and the usage of *Commonality* and *Connectivity* to cope with this. It is seen that *Kraken* spawns 10% more containers for *Media Service* and 6% more for *Hotel Reservation* and *Social Network*. This may be due to *Media Service* having higher path unpredictability than *Hotel Reservation* (Table 2) as well as lower slack per function than *Social Network* (Figure 7). From Figure 16b, it is observed that *Oracle*, being clairvoyant, spawns containers in accordance with the peaks and valleys of the request arrival trace. *Kraken*, while spawning more containers, also is seen to lag behind the trend of the trace due to load prediction errors.

Performance under Sparse Load: Analysis of logs collected from the Azure cloud platform [42] shows request volumes that are much lighter (average of 2 requests/hour) than those of the traces we have considered. Moreover, more than 40% of requests show significant variability in inter-arrival times. To deal with such traces, we modified *Kraken*'s load prediction model to predict future request arrival times, owing to the sparse nature of the trace. We also spawn containers much more in advance than the predicted arrival time and also keep them alive for at least a minute before evicting them from memory, to account for arrival unpredictability. It is seen that *Kraken* meets the SLOs for all requests from the lightly-loaded trace over 18 hours while averaging 0.85 memory-resident containers at any given second[3]. Other

---

[3]These results are not shown in any graph.

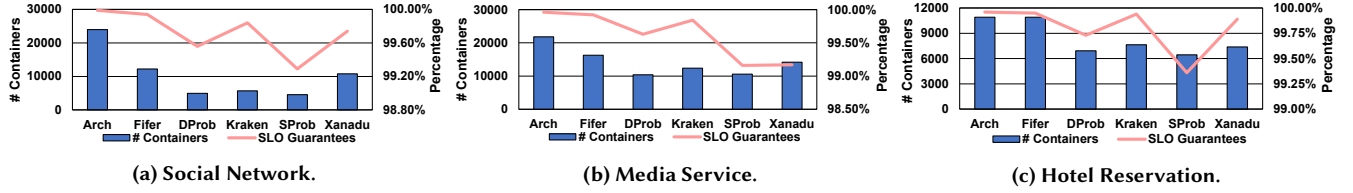(a) Social Network.   (b) Media Service.   (c) Hotel Reservation.

Figure 14: Simulator: Comparison of Total Number of Containers spawned VS SLOs satisfied by each policy. The Primary Y-Axis denotes the number of containers spawned, The secondary Y-axis indicates the percentage of SLOs met and the X-axis represents each policy.
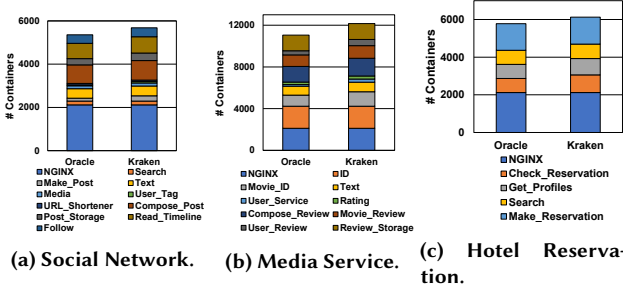

(a) Social Network.   (b) Media Service.   (c) Hotel Reservation.

Figure 15: Simulator: Comparison of Function-wise Breakdown of Containers spawned by *Kraken* and *Oracle*.

(a) E2E Response Time Breakdown.   (b) Containers spawned over time.
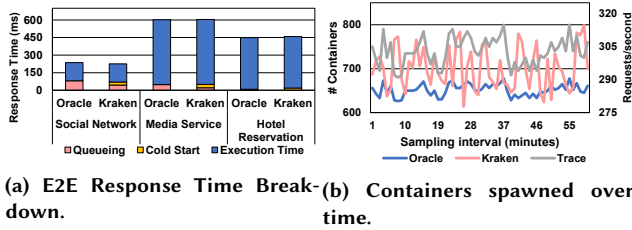
Figure 16: Simulator: Comparison of End-to-End (E2E) Response Times and Containers Spawned Over Time (60 minutes) of *Kraken* and *Oracle*.

Trace	Arch	Fifer	Kraken	Xanadu	Comm Only	Conn Only
Wiki	(99.91%, 2737)	(99.90%, 2092)	(99.86%, 1396)	(99.66%, 1737)	(99.78%,)	(99.75%,)
Twitter	(99.72%, 45,107)	(99.63%, 34,210)	(99.50%, 22,377)	(99.10%, 25,132)	(99.22%,)	(99.15%,)

Table 7: Simulator: Comparing (% SLO met,# Containers Spawned) against Existing Policies after Varying the Target SLOs.

existing policies such as *Arch* and *Fifer* exhibit similar performance and resource usage when their prediction models and keep-alive times are similarly adjusted. *Xanadu*, on the other hand, while having 0.74 memory-resident containers per second, suffers from 55% SLO Violations on average across all applications as a result of MLP mispredictions whose effects are exacerbated in this scenario, due to low request volume. **Varying SLO:** Table 7 shows the SLO guarantees and number of containers spawned for existing policies as well as *Comm Only* and *Conn Only*, when the SLO is reduced from 1000ms to a value 30% higher than the response time of the slowest workflow in each application. The resultant SLOs are 500ms, 910ms and 809ms for *Social Network*, *Media Service* and *Hotel Reservation* respectively. Reducing the SLO, in turn, can potentially reduce the batch sizes of functions as well. Moreover, the reduced SLO target results in increased SLO violations across all policies. However, *Kraken* is able to

maintain at least 99.5% SLO guarantee and spawns 50%, 34% and 15% less containers compared to *Arch*, *Fifer* and *Xanadu*, respectively. It can be seen that the difference in SLO compliance between *Kraken*, *Comm Only*, and *Conn Only* increases due to the reduced target SLO. This difference, in terms of percent of SLO violations, changes from being at most 0.1% to being between 0.1 to 0.35%. This is a result of *Kraken* being more resilient at the tail of the response time distribution as it uses both *Commonality* and *Connectivity* while spawning containers. In comparison, *Comm Only* and *Conn Only* fail to spawn enough containers for each important function as they do not consider both these parameters, resulting in increased tail latency and exacerbates the SLO violations.

7 Concluding Remarks

Adopting serverless functions for executing microservice-based applications introduces critical inefficiencies in terms of scheduling and resource management for the cloud provider, especially when deploying Dynamic DAG Applications. Towards addressing these challenges, we design and evaluate *Kraken*, a DAG workflow-aware resource management framework, for efficiently running such applications by utilizing minimum resources, while remaining SLO-compliant. *Kraken* employs proactive weighted scaling of functions, where the weights are calculated using function invocation probabilities and other parameters pertaining to the application's DAG structure. Our experimental evaluation on a 160-core cluster using *Deathstarbench* workload suite and real-world traces demonstrate that *Kraken* spawns up to 76% fewer containers, thereby improving container utilization and cluster-wide energy savings by up to 4× and 48%, respectively, compared to state-of-the art schedulers employed in serverless platforms.

8 Acknowledgement

References

[1] [n.d.]. Twitter Stream traces. https://archive.org/details/twitterstream. Accessed: 2020-05-07.

[2] 2019. Airbnb AWS Case Study. https://aws.amazon.com/solutions/case-studies/airbnb/.

[3] 2019. Provisioned Concurrency. https://docs.aws.amazon.com/lambda/latest/dg/configuration-concurrency.html.

[4] 2020. Amazon States Language. https://docs.aws.amazon.com/step-functions/latest/dg/concepts-amazon-states-language.html.

[5] 2020. AWS Lambda. Serverless Functions. https://aws.amazon.com/lambda/.

[6] 2020. Azure Durable Functions. https://docs.microsoft.com/en-us/azure/azure-functions/durable.

[7] 2020. hey HTTP Load Testing Tool. https://github.com/rakyll/hey.

[8] 2020. IBM-Composer. https://cloud.ibm.com/docs/openwhisk?topic=cloud-functions-pkg_composer.

[9] 2020. Kubernetes. https://kubernetes.io/.

[10] 2020. Microsoft Azure Serverless Functions. https://azure.microsoft.com/en-us/services/functions/.

[11] 2020. OpenFaaS. https://www.openfaas.com/.

[12] 2020. Prometheus. https://prometheus.io/.

[13] 2021. AWS Lambda Cold Starts. https://mikhail.io/serverless/coldstarts/aws/.

[14] 2021. Azure Functions Cold Starts. https://mikhail.io/serverless/coldstarts/azure/.

[15] 2021. Expedia Case Study - Amazon AWS. https://mikhail.io/serverless/coldstarts/azure/.

[16] Feb 24, 2020. Intel Power Gadget. https://github.com/sosy-lab/cpu-energy-meter.

[17] February 2018. Google Cloud Functions. https://cloud.google.com/functions/docs/.

[18] Istemi Ekin Akkus et al. 2018. SAND: Towards High-Performance Serverless Computing. In *ATC*.

[19] Mamoun Awad, Latifur Khan, and Bhavani Thuraisingham. 2008. Predicting WWW surfing using multiple evidence combination. *The VLDB Journal* 17, 3 (2008), 401–417.

[20] M. A. Awad and I. Khalil. 2012. Prediction of User's Web-Browsing Behavior: Application of Markov Model. *IEEE Transactions on Systems, Man, and Cybernetics, Part B (Cybernetics)* 42, 4 (2012), 1131–1142. https://doi.org/10.1109/TSMCB.2012.2187441

[21] Ron Begleiter, Ran El-Yaniv, and Golan Yona. 2004. On Prediction Using Variable Order Markov Models. *Journal of Artificial Intelligence Research* 22 (2004), 385–421.

[22] Marc Brooker, Andreea Florescu, Diana-Maria Popa, Rolf Neugebauer, Alexandru Agache, Alexandra Iordache, Anthony Liguori, and Phil Piwonka. 2020. Firecracker: Lightweight Virtualization for Serverless Applications. In *NSDI*.

[23] Jyothi Prasad Buddha and Reshma Beesetty. 2019. Step Functions. In *The Definitive Guide to AWS Application Integration*. Springer.

[24] James Cadden, Thomas Unger, Yara Awad, Han Dong, Orran Krieger, and Jonathan Appavoo. 2020. SEUSS: skip redundant paths to make serverless fast. In *Proceedings of the Fifteenth European Conference on Computer Systems*. 1–15.

[25] Joao Carreira, Pedro Fonseca, Alexey Tumanov, Andrew Zhang, and Randy Katz. 2019. Cirrus: A Serverless Framework for End-to-End ML Workflows. In *Proceedings of the ACM Symposium on Cloud Computing* (Santa Cruz, CA, USA) *(SoCC '19)*. Association for Computing Machinery, New York, NY, USA, 13–24. https://doi.org/10.1145/3357223.3362711

[26] Benjamin Carver, Jingyuan Zhang, Ao Wang, and Yue Cheng. 2019. In search of a fast and efficient serverless dag engine. In *2019 IEEE/ACM Fourth International Parallel Data Systems Workshop (PDSW)*. IEEE, 1–10.

[27] Nilanjan Daw, Umesh Bellur, and Purushottam Kulkarni. 2020. Xanadu: Mitigating cascading cold starts in serverless function chain deployments. In *Proceedings of the 21st International Middleware Conference*. 356–370.

[28] Paul A Gagniuc. 2017. *Markov chains: From Theory to Implementation and Experimentation*. John Wiley & Sons.

[29] Yu Gan, Yanqi Zhang, Dailun Cheng, Ankitha Shetty, Priyal Rathi, Nayan Katarki, Ariana Bruno, Justin Hu, Brian Ritchken, Brendon Jackson, et al. 2019. An open-source benchmark suite for microservices and their hardware-software implications for cloud & edge systems. In *Proceedings of the Twenty-Fourth International Conference on Architectural Support for Programming Languages and Operating Systems*. 3–18.

[30] Arpan Gujarati, Sameh Elnikety, Yuxiong He, Kathryn S. McKinley, and Björn B. Brandenburg. 2017. Swayam: Distributed Autoscaling to Meet SLAs of Machine Learning Inference Services with Resource Efficiency. In *USENIX Middleware Conference*.

[31] Jashwant Raj Gunasekaran, Prashanth Thinakaran, Mahmut Taylan Kandemir, Bhuvan Urgaonkar, George Kesidis, and Chita Das. 2019. Spock: Exploiting Serverless Functions for SLO and Cost Aware Resource Procurement in Public Cloud. In *2019 IEEE 12th International Conference on Cloud Computing (CLOUD)*. 199–208. https://doi.org/10.1109/CLOUD.2019.00043

[32] Jashwant Raj Gunasekaran, Prashanth Thinakaran, Nachiappan C Nachiappan, Mahmut Taylan Kandemir, and Chita R Das. 2020. Fifer: Tackling Resource Underutilization in the Serverless Era. In *Proceedings of the 21st International Middleware Conference*. 280–295.

[33] Eric Jonas, Johann Schleier-Smith, Vikram Sreekanti, Chia-Che Tsai, Anurag Khandelwal, Qifan Pu, Vaishaal Shankar, Joao Carreira, Karl Krauth, Neeraja Yadwadkar, et al. 2019. Cloud programming simplified: A berkeley view on serverless computing. *arXiv preprint arXiv:1902.03383* (2019).

[34] Ram Srivatsa Kannan, Lavanya Subramanian, Ashwin Raju, Jeongseob Ahn, Jason Mars, and Lingjia Tang. 2019. GrandSLAm: Guaranteeing SLAs for Jobs in Microservices Execution Frameworks. In *EuroSys*.

[35] Kate Keahey, Jason Anderson, Zhuo Zhen, Pierre Riteau, Paul Ruth, Dan Stanzione, Mert Cevik, Jacob Colleran, Haryadi S. Gunawi, Cody Hammock, Joe Mambretti, Alexander Barnes, François Halbach, Alex Rocha, and Joe Stubbs. 2020. Lessons Learned from the Chameleon Testbed. In *Proceedings of the 2020 USENIX Annual Technical Conference (USENIX ATC '20)*. USENIX Association.

[36] Bernhard Korte and Jens Vygen. 2018. Bin-Packing. In *Combinatorial Optimization*. Springer, 489–507.

[37] Jörn Kuhlenkamp, Sebastian Werner, and Stefan Tai. 2020. The ifs and buts of less is more: a serverless computing reality check. In *2020 IEEE International Conference on Cloud Engineering (IC2E)*. IEEE, 154–161.

[38] Anup Mohan, Harshad Sane, Kshitij Doshi, Saikrishna Edupuganti, Naren Nayak, and Vadim Sukhomlinov. 2019. Agile cold starts for scalable serverless. In *11th {USENIX} Workshop on Hot Topics in Cloud Computing (HotCloud 19)*.

[39] Edward Oakes, Leon Yang, Dennis Zhou, Kevin Houck, Tyler Harter, Andrea Arpaci-Dusseau, and Remzi Arpaci-Dusseau. 2018. SOCK: Rapid Task Provisioning with Serverless-Optimized Containers. In *USENIX ATC*.

[40] Haoran Qiu, Subho S Banerjee, Saurabh Jha, Zbigniew T Kalbarczyk, and Ravishankar K Iyer. 2020. {FIRM}: An Intelligent Fine-grained Resource Management Framework for SLO-Oriented Microservices. In *14th {USENIX} Symposium on Operating Systems Design and Implementation ({OSDI} 20)*. 805–825.

[41] Mohammad Shahrad, Jonathan Balkind, and David Wentzlaff. 2019. Architectural implications of function-as-a-service computing. In *Proceedings of the 52nd Annual IEEE/ACM International Symposium on Microarchitecture*. 1063–1075.

[42] Mohammad Shahrad, Rodrigo Fonseca, Íñigo Goiri, Gohar Chaudhry, Paul Batum, Jason Cooke, Eduardo Laureano, Colby Tresness, Mark Russinovich, and Ricardo Bianchini. 2020. In *2020 {USENIX} Annual Technical Conference ({USENIX}{ATC} 20)*. 205–218.

[43] Paulo Silva, Daniel Fireman, and Thiago Emmanuel Pereira. 2020. Prebaking Functions to Warm the Serverless Cold Start. In *Proceedings of the 21st International Middleware Conference*. 1–13.

[44] Arjun Singhvi, Kevin Houck, Arjun Balasubramanian, Mohammed Danish Shaikh, Shivaram Venkataraman, and Aditya Akella. 2019. Archipelago: A scalable low-latency serverless platform. *arXiv preprint arXiv:1911.09849* (2019).

[45] Davide Taibi, Nabil El Ioini, Claus Pahl, and Jan Raphael Schmid Niederkofler. 2020. Patterns for Serverless Functions (Function-as-a-Service): A Multivocal Literature Review.. In *CLOSER*. 181–192.

[46] Ali Tariq, Austin Pahl, Sharat Nimmagadda, Eric Rozner, and Siddharth Lanka. 2020. Sequoia: Enabling quality-of-service in serverless computing. In *Proceedings of the 11th ACM Symposium on Cloud Computing*. 311–327.

[47] Prashanth Thinakaran, Jashwant Raj Gunasekaran, Bikash Sharma, Mahmut Taylan Kandemir, and Chita R. Das. 2017. Phoenix: A Constraint-Aware Scheduler for Heterogeneous Datacenters. In *2017 IEEE 37th International Conference on Distributed Computing Systems (ICDCS)*. 977–987. https://doi.org/10.1109/ICDCS.2017.262

[48] Prashanth Thinakaran, Jashwant Raj Gunasekaran, Bikash Sharma, Mahmut Taylan Kandemir, and Chita R. Das. 2019. Kube-Knots: Resource Harvesting through Dynamic Container Orchestration in GPU-based Datacenters. In *2019 IEEE International Conference on Cluster Computing (CLUSTER)*. 1–13. https://doi.org/10.1109/CLUSTER.2019.8891040

[49] Guido Urdaneta, Guillaume Pierre, and Maarten Van Steen. 2009. Wikipedia workload analysis for decentralized hosting. *Computer Networks* (2009).

[50] Liang Wang, Mengyuan Li, Yinqian Zhang, Thomas Ristenpart, and Michael Swift. 2018. Peeking Behind the Curtains of Serverless Platforms. In *ATC*.

[51] Hailong Yang, Quan Chen, Moeiz Riaz, Zhongzhi Luan, Lingjia Tang, and Jason Mars. 2017. PowerChief: Intelligent power allocation for multi-stage applications to improve responsiveness on power constrained CMP. In *Computer Architecture News*.

[52] Yiming Zhang, Jon Crowcroft, Dongsheng Li, Chengfen Zhang, Huiba Li, Yaozheng Wang, Kai Yu, Yongqiang Xiong, and Guihai Chen. 2018. KylinX: a dynamic library operating system for simplified and efficient cloud virtualization. In *2018 USENIX Annual Technical Conference*. 173–186.